International Journal of Nanomedicine

Dovepress
open access to scientific and medical research

Open Access Full Text Article

ORIGINAL RESEARCH

Dual-Stimuli-Responsive Gut Microbiota-Targeting Nitidine Chloride-CS/PT-NPs Improved Metabolic Status in NAFLD

Jianmei Lu[1,2,*], Yongzhu Zeng[1,*], Huashuai Zhong[1], Wei Guo[1], Yuyan Zhang[1], Wanting Mai[3], Yucui Qin[4], Xiaodan Su[3], Bo Zhang[5], Weisen Wu[1], Yu Zhu[1], Qiujie Huang[6], Yong Ye[1,7–9]

[1]Department of Pharmacy, Guangxi Medical University, Nanning, People's Republic of China; [2]The Second Nanning People's Hospital, Nanning, People's Republic of China; [3]The Second Affiliated Hospital of Guangxi Medical University, Nanning, People's Republic of China; [4]Maternity and Child Health Care of Guangxi Zhuang Autonomous Region, Nanning, People's Republic of China; [5]Scientific Research Center, Guilin Medical University, Guilin, People's Republic of China; [6]Department of Pharmacy, Guangxi University of Traditional Chinese Medicine, Nanning, People's Republic of China; [7]Guangxi Key Laboratory of Bioactive Molecules Research and Evaluation, Nanning, People's Republic of China; [8]Guangxi Key Laboratory of Pharmaceutical Precision Detection and Screening, Nanning, People's Republic of China; [9]Key Laboratory of Micro-Nanoscale Bioanalysis and Drug Screening of Guangxi Education Department, Nanning, People's Republic of China

*These authors contributed equally to this work

Correspondence: Qiujie Huang, Department of Pharmacy, Guangxi University of Traditional Chinese Medicine, Nanning, People's Republic of China, Email hqj8@163.com; Yong Ye, Department of Pharmacy, Guangxi Medical University, Nanning, People's Republic of China, Email yong-ye@163.com

Background and Purpose: Nitidine chloride (NC) is a botanical drug renowned for its potent anti-inflammatory, antimalarial, and hepatocellular carcinoma-inhibiting properties; however, its limited solubility poses challenges to its development and application. To address this issue, we have devised a colon-targeted delivery system (NC-CS/PT-NPs) aimed at modulating the dysbiosis of the gut microbiota by augmenting the interaction between NC and the intestinal microbiota, thereby exerting an effect against nonalcoholic fatty liver disease.

Methods: The NC-CS/PT-NPs were synthesized using the ion gel method. Subsequently, the particle size distribution, morphology, drug loading efficiency, and release behavior of the NC-CS/PT-NPs were characterized. Furthermore, the impact of NC-CS/PT-NPs on non-alcoholic fatty liver disease (NAFLD) induced by a high-fat diet (HFD) in mice was investigated through serum biochemical analysis, ELISA, and histochemical staining. Additionally, the influence of NC-CS/PT-NPs on intestinal microbiota was analyzed using 16S rDNA gene sequencing.

Results: The nanoparticles prepared in this study have an average particle size of (255.9±5.10) nm, with an encapsulation rate of (72.83±2.13) % and a drug loading of (4.65±0.44) %. In vitro release experiments demonstrated that the cumulative release rate in the stomach and small intestine was lower than 22.0%, while it reached 66.75% in the colon. In vivo experiments conducted on HFD-induced NAFLD mice showed that treatment with NC-CS/PT-NPs inhibited weight gain, decreased serum aspartate aminotransferase (AST), Alanine aminotransferase (ALT) and lipid levels, improved liver and intestinal inflammation, and altered the diversity of gut microbiota in mice.

Conclusion: This study provides new evidence for the treatment of NAFLD through the regulation of gut microbiota using active ingredients from traditional Chinese medicine.

Keywords: nanoparticles, colonic targeting, metabolic disorders, gut microbiota

Introduction

Non-alcoholic fatty liver disease (NAFLD) is one of the most common forms of chronic liver disease throughout the world.[1,2] It encompasses a spectrum ranging from simple steatosis to nonalcoholic steatohepatitis (NASH), which is a more aggressive form of the disease that can progress to liver fibrosis, cirrhosis, and life-threatening complications.[3] The global incidence of NAFLD has been steadily increasing, with a growth rate of 0.7% per year between 1990 and

Received: 4 December 2023
Accepted: 27 February 2024
Published: 8 March 2024

2019. In 2019, the prevalence rate reached approximately 37%. Notably, North and South America had the highest prevalence rates at 35%, while Asia and Europe exhibited a prevalence rate of 28%.[4] China has particularly high rates of NAFLD, with an overall prevalence rate of 29.6% from 1999 to 2018. This makes China the country with the highest prevalence, incidence, and annual NAFLD-related mortality rate in Asia. It is projected that by 2030, China will experience the largest increase in NAFLD prevalence globally, leading to a significant rise in the economic burden associated with the disease.[5] The current treatment strategies for NAFLD include rational diet and exercise intervention, as well as combined drug treatment. However, due to the complex pathogenesis of NAFLD, there is still a lack of specific drugs.[6,7] Previous research has shown that the transition from steatosis to steatosis hepatitis is influenced by genetic predisposition, insulin resistance, abnormal lipid metabolism, and mitochondrial dysfunction.[2] Despite these findings, a comprehensive understanding of the underlying mechanisms is still lacking, which hinders the development of effective treatments for NAFLD. Interestingly, the gut microbiota has been identified as a crucial factor in the pathophysiology of metabolic disorders, including NAFLD, through the gut-liver axis.[8–10] Several clinical studies from past years demonstrated that gut microbiome signature also exists in human NAFLD. This indicates that gut microbiota may be a promising therapeutic target for NAFLD.

Nitidine chloride (NC) is a key active ingredient found in *Zanthoxylum nitidum* (Roxb.) DC., a commonly used Chinese herbal medicine. *Z. nitidum* is known for its various medicinal properties, including promoting blood circulation, relieving pain, and detoxifying the body.[11] Numerous modern pharmacological studies have highlighted the impressive biological activities of nitidine chloride, such as liver protection, anti-liver cancer effects, anti-inflammatory properties, and its potential in treating conditions like colitis, malaria, and osteoporosis.[12] However, the limited water solubility and low bioavailability of NC pose challenges to its clinical application.[13] Therefore, it is crucial to explore the potential of NC formulations in reducing drug toxicity, improving solubility, and ultimately facilitating its use in clinical settings.

The nanoparticle drug delivery system offers several advantages, including high bioavailability, good system stability, high drug loading, long blood circulation, and a long selective distribution half-life in organs and tissues.[14–16] Oral administration is particularly beneficial in enhancing the absorption of nanoparticles, especially in inflammatory or ulcerated tissues. One effective approach for targeted delivery to the colon is through the use of oral colon targeted delivery systems (OCDDS), which can deliver drugs directly to the colon site with precise localization. Currently, OCDDS carriers primarily consist of natural polysaccharides and synthetic azo polymers, such as gum, sodium alginate, chitosan, et cetera.[17,18] Chitosan and pectin, for instance, can serve as prebiotics to regulate intestinal microorganisms and improve hyperlipidemia and obesity. By utilizing the ionic interaction between NH^{3+} of chitosan and $–COO^{–}$ of pectin, it is possible to form polyelectrolyte composite nanoparticles that exhibit responsiveness to the intestinal microbiome and pH.[19] Therefore, in this study, we have specifically chosen chitosan and pectin as carriers that are tailored to the physiological conditions of regions abundant in gut microbiota. These carriers form polyelectrolyte complexes that demonstrate dual-stimulus-responsiveness, namely pH sensitivity and degradation by gut microbiota.

In this study, we designed a pH/gut microbiota responsive system of NC nanoparticles (NC-CS/PT-NPs), and explored whether NC-CS/PT-NPs could treat high-fat diet-induced NAFLD by regulating gut microbiota.

Materials and Methods

Materials

Chitosan (deacetylation degree 75%) and Tripolyphosphate were purchased from Aladdin (Shanghai, China). Pectin was purchased from Sigma Aldrich (St Louis, MO, USA). Nitidine chloride was obtained from Chengdu Ruide Fensi Technology Co., Ltd (Chengdu, China). Enzyme-linked immunosorbent assay (ELISA) kits for interleukin-1β (IL-1β), interleukin-6 (IL-6), tumor necrosis factor-α (TNF-α), and monocyte chemotactic protein-1 (MCP-1) were purchased from Shanghai Kexing Trading Co., Ltd (Shanghai, China). IHC Caspase-8, keap-1, Nrf2, OH-1 primary antibody were purchased from Proteintech Group, Inc (Wuhan, China). All other reagents and kits were of analytical grade. All water used in the study was freshly double distilled.

Preparation of NC-Loaded CS/PT Nanoparticles

According to a previously described method,[19] chitosan (2.0 mg/mL) was dissolved in acetate buffers with pH values of 4.0, 4.5, 5.0, and 5.5. Pectin (2.0 mg/mL), tripolyphosphate (2.0 mg/mL), and Nitidine chloride were separately dissolved in water. 4 mL of Nitidine chloride solution, 6 mL of TPP solution, and 6 mL of pectin solution were successively added to nine milliliters of chitosan solution (total volume of 25 mL) and stirred at room temperature for 30 min. The precipitate was separated by ultracentrifugation at 4000 rpm for 20 min using a Table-type Low-speed Centrifuge (TD5A-WS, China), washed with deionized water, and then freeze-dried. Each precipitate was weighed to determine the weight of the solid complex.

Determination of Encapsulation Efficiency

The unbound NC in the supernatant and the weakly adsorbed NC on the surface of the NC-CS/PT-NPs were collected by centrifugation and washed off twice with methanol, respectively. The amount of NC in the methanol rinse and the supernatant were both analyzed to determine the total unbound NC by injecting 20 μL on to an HPLC system. The amount of NC in the samples was obtained by comparing peak area obtained with those from a standard curve treated similarly. The percentage of encapsulated NC was calculated as follows:

$$\%\text{Encapsulation Efficiency} = \frac{\text{Total NC added} - \text{unbound NC}}{\text{Total NC added}} \times 100\%$$

Characterization of NC-CS/PT-NPs

Particle Sizes and Zeta Potentials of NC-CS/PT-NPs

The particle sizes, polydispersity indexes (PDIs), and zeta potentials of NC-CS/PT-NPs were measured by dynamic light scattering (DLS) (Nano ZS, Malvern, UK).

Transmission Electron Microscopy (TEM)

The morphology of the NC-CS/PT-NPs was analyzed using a transmission electron microscope (TEM) (HTACHI, H-7650, Japan). After dilution, the NC-CS/PT-NPs were deposited onto copper grids with 200-mesh carbon membranes and then dried.

Differential Scanning Calorimetry (DSC)

To characterize the crystal form of NC-CS/PT-NPs, we performed DSC using the DSC1 instrument from Mettler-Toledo International Inc., Switzerland. Approximately 20 mg of the samples were sealed in an alumina crucible and heated from 30 to 300 °C at a linear heating rate of 10°C /min.

X-Ray Diffraction (XRD)

To investigate the crystallinity of NC-CS/PT-NPs, PXRD analysis was conducted using the X'pert Pro-MPD X-ray diffractometer (Rigaku Corporation, Japan) with the following parameters: scanning speed of 5°/min, 2θ range from 5° to 55°, and a scanning increment of 0.02°.

Fourier Transforms Infrared Spectroscopy (FTIR)

The sample was prepared by freeze-drying and grinding it with potassium bromide. The resulting mixture was then extruded to form a disc. Nicolet IS20 FITC spectrometer scans (Thermo Fisher Scientific, USA) were obtained using three runs, covering the range of 400 to 4000 cm^{-1}.

In vitro Release Analysis

The in vitro release of NC from NC, NC-CS/PT-NPs was investigated using dialysis analysis. Cellulose acetate dialysis bags with a molecular weight cutoff of 8000–14,000 Da (Shanghai Yuanye Biotechnology Co., Ltd, China) were used. 3 mL of NC and NC-CS/PT-NPs were separately added to different dialysis bags and suspended in HCl (pH 2.0, 20 mL) for 2 h to simulate gastric transit. Subsequently, the dialysis bag was suspended in phosphate buffer (pH 6.8, 20 mL) for 4 h to mimic the conditions of the small intestine. Finally, the dialysis bag was incubated in phosphate buffer (pH 7.4, 20 mL, containing 80% rat cecal filtrate) for 14 h at 37 °C with agitation to simulate the colon conditions. Samples were

collected at the end of each simulated duration, and the supernatants obtained after centrifugation were used for NC assay. The release study was conducted in triplicate for each time point. TEM images and size distribution analysis of NC-CS/PT-NPs were performed after exposure to different simulated biological fluids to confirm the pH and microbial sensitivity of the delivery systems.

Animal Studies

In vivo Anti-Nonalcoholic Fatty Liver Disease Effect

All animal experiments were conducted with the approval of the Animal Ethics Committee of Guangxi Medical University and in compliance with the Guidelines for the Care and Use of Laboratory Animals. Male C57 mice weighing between 18–22 g were obtained from Guangxi Medical University Animal Centre (Guangxi, China). Ethic approval for animal experiments was obtained from the Guangxi Medical University Laboratory Animal Center (Certificate No. SYXK2020-003). Animal's welfare was ensured during whole animal experiments.

Establishment of the Nonalcoholic Fatty Liver Disease Model and Drug Treatment

C57 mice were housed in the SPF grade rooms and had free access to food and water. C57 mice were randomly separated into two groups at the first seventeen weeks: the normal chow diet controls (NCD, 12 animals) and high-fat-diet models (HFD, 48 animals). Then, animals of high-fat-diet group were randomly reallocated into four groups: HFD group (distilled water, by gavage), NC group (8 mg/kg/day, by gavage), NC-CS/PT-NPs group (containing NC 8 mg/kg/day, by gavage), and Silymarin group (200 mg/kg/day, by gavage), and the NCD group was also administered the same volume of distilled water for another 4 weeks. During the entire experiment, body weight of C57 mice was measured weekly. At the end of experiment, mice were humanely sacrificed; liver, cecum and colon contents were collected. The liver were weighted and collected at −80 °C for further analysis. Parts of liver were used for histological and IHC, cecum and colon contents were used for SCFAs measurement.

Plasma Biochemical Assays

Blood samples were obtained from the mice and centrifuged at 3000 rpm for 20 min to separate the serum. The levels of total cholesterol (TG), triglyceride (TC), aspartate aminotransferase (AST), Alanine aminotransferase (ALT) and low-density lipoprotein (LDL) were determined using a kit according to the instructions provided by Nanjing Jiancheng Bioengineering Research Institute, China.

Histological Staining

The livers and colons of mice were removed, flushed with PBS, fixed in 10% paraffin, and then cut into 4 μm sections for subsequent staining. Hematoxylin and eosin staining (HE) was used to analyze morphometric lesions in the liver and colon. Masson staining and Oil red O staining (ORO) were performed to assess fat accumulation in the hepatic tissue.

Immunohistochemical Staining (IHC)

The liver sections were deparaffinized using xylene, rehydrated with graded alcohol, and subsequently washed in ultrapure water for 5 min. Next, the sections were heated at 100 °C for 10 min to facilitate antigen retrieval. The tissues were then incubated in 5% goat serum for a period of 20–60 min. Following this, they were incubated with primary antibodies (The dilution ratio of all antibodies was 1:200) for 1 h at 37 °C. Finally, the immunoreaction was visualized by incubating with a secondary antibody for 15 min. The expression levels of Caspase-8, Keap-1, Nfr2 and OH-1 proteins in liver tissues were detected using IHC method. The IHC integral density of each group of proteins was quantitatively analyzed using Image software.

Determination of Pro-Inflammatory Cytokines in Liver Tissue

Liver tissues from different groups were weighed and homogenized at 4 °C. The homogenized samples were then centrifuged at 3000 rpm for 20 min, and the resulting supernatant was collected. ELISA kits were used to measure the levels of Interleukin-6 (IL-6), Interleukin-1β (IL-1β), Tumor necrosis factor (TNF-α), and Monocyte chemotactic protein-1 (MCP-1) in the supernatant.

Gut Inflammation and Histological Analysis

Colon tissues were homogenized at 4 °C with normal saline at a ratio of 1:9 (mass to volume). After centrifugation at 3000 rpm for 20 min, the supernatant was collected and used to measure the levels of IL-6, IL-1β, MCP-1 and TNF-α using an ELISA kit.

Mouse Intestine 16S Ribosomal DNA (16 S rDNA) Analysis

The feces from each group were collected in aseptic conditions after treatment with NC-CS/PT-NPs. Total genomic DNA was extracted from mice feces using the MagPure Soil DNA KF Kit (Magan) according to the manufacturer's instructions. DNA concentration and integrity were determined using the NanoDrop 2000 (Thermo Fisher Scientific, USA). The diversity of gut bacteria in mice feces was analyzed through 16S rDNA gene analysis. The V3-V4 regions of the 16S rDNA gene were amplified using the universal primers 343F (5'-TACGGRAGGCAGCAG-3') and 798R (5'-AGGGTATCTAATCCT-3') and purified using AMPure XP beads (Agencourt). Sequencing was performed on an Illumina NovaSeq 6000 with 250 bp paired-end reads (Illumina Inc., San Diego, CA; OE Biotech Company; Shanghai, China). The representative read of each ASV was selected using the QIIME2 software package (2020.11) after quality filtering.

Statistical Analysis

All data were expressed as mean ± standard deviation (SD). Statistical analysis was performed in GraphPad Prism Software Version 8.0 (GraphPad, San Diego, CA) using unpaired student's test. Statistical significance was set at $p<0.05$.

Results

Preparation of NC-CS/PT-NPs

The average particle size of NC-CS/PT-NPs was determined to be 255.9 ± 5.10 nm with a PDI of 0.199 ± 0.01 (Figure 1a). The corresponding average Zeta potentials of NC-CS/PT-NPs were measured to be 29.30 ± 0.77 mV (Figure 1b). The encapsulating efficiency was found to be (72.83 ± 2.13) %, and the drug loading was (4.65 ± 0.44) %. The size, surface morphology, and structure of NC-CS/PT-NPs were examined using TEM. The TEM image (Figure 1c) showed that NC-CS/PT-NPs exhibited a predominantly spherical shape with a uniform distribution and no adhesion phenomenon.

Crystalline State

The results of the DSC analysis are presented in Figure 1d. The CS/PT-NPs, NC-CS/PT-NPs, and the physical mixture of NC-CS/PT-NPs and NC exhibited noticeable endothermic peaks at approximately 165 °C. It was observed that the endothermic peaks of CS/PT-NPs were more pronounced compared to those of the physical mixture. Moreover, all the samples displayed a broad range of endothermic peaks ranging from 50 to 120 °C, which can be attributed to the presence of residual moisture.

To confirm the crystalline form, XRD analysis was performed. As depicted in Figure 1e, the diffraction pattern of NC exhibited a highly crystalline nature, evident from the numerous peaks observed. The presence of numerous peaks in the diffraction pattern of the physical mixture of NC-CS/PT-NPs and NC can be solely attributed to NC, indicating that CS/PT-NPs had no influence on the crystalline transition of the drug.

Intermolecular Interactions

The characteristic peaks of NC are observed at 1300 cm^{-1}, 2300 cm^{-1}, and 5250 cm^{-1} in Figure 1f. In NC-CS/PT-NPs, the characteristic peaks at 1300 cm^{-1} and 2300 cm^{-1} of NC are shifted and weakened, while the peak at 5250 cm^{-1} disappears. This suggests that there are no new chemical bonds formed between the physical mixtures, but rather the formation of a complex instead of a new compound. Comparing CS/PT-NPs with NC-CS/PT-NPs, the characteristic peak of NC at 1300 cm^{-1} is still present in NC-CS/PT-NPs, indicating that NC is encapsulated within the nanoparticles. This implies that the components of NC-CS/PT-NPs form hydrogen bonds with each other or undergo the formation of van der Waals forces.

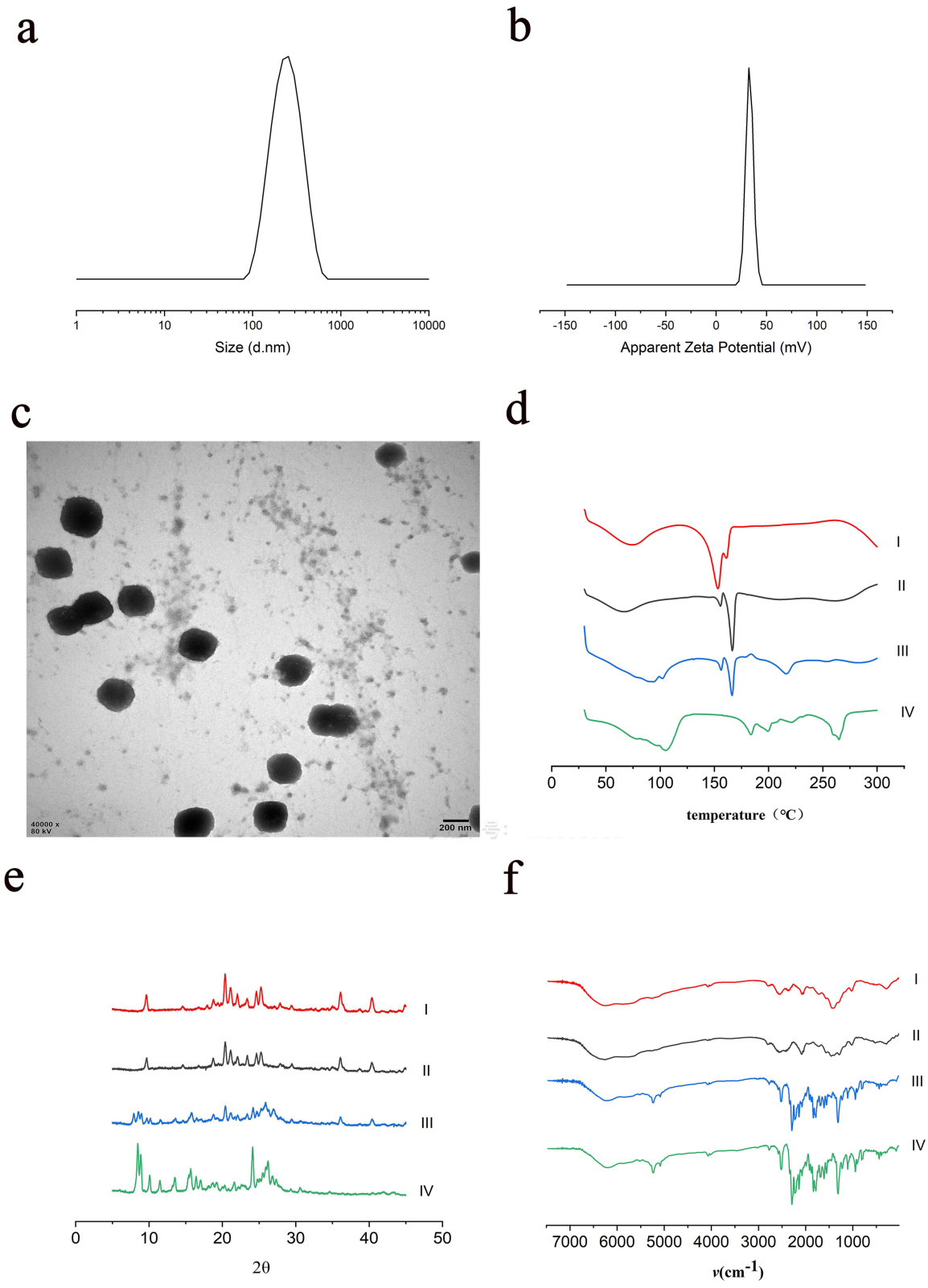

Figure 1 Characterization of NC-CS/PT-NPs. (**a**) Representative diagram of particle size. (**b**) Zeta potential. (**c**) Representative image of morphology of NC-CS/PT-NPs (200 nm). (**d**) Overlay of DSC thermogram of NC, NC-CS/PT-NPs, CS/PT-NPs, CS/PT-NPs and NC physical mixture. (**e**) XRD overlay spectra on NC, NC-CS/PT-NPs, CS/PT-NPs, CS/PT-NPs and NC physical mixture. (**f**) FT-IR spectra of NC, NC-CS/PT-NPs, CS/PT-NPs, CS/PT-NPs and NC physical mixture.
Notes: I NC-CS/PT-NPs. II: CS/PT-NPs. III: CS/PT-NPs and NC physical mixture. IV: NC.

In vitro Dissolution Study of NC-CS/PT-NPs

The study investigated the sustained release profile of NC from nanoparticles by examining its behavior in different dissolution media. After oral administration, the drug passes through the stomach (pH: 1.5, 2 h), then traverses the small intestine (pH: 6.8, 4 h), and finally arrives at the large intestine (pH: 7.4, rich in gut-microbiota, 14 h). The study specifically examined the release of NC in simulated gastric fluid (SGF, pH 1.5), simulated intestinal fluid (SIF, pH 6.8), and simulated colon fluid (SCF, pH 7.4, 20% rat caeca filtration). Burst release was not observed in SIF or SGF, which suggests that the positively charged NC could form a strong electrostatic interaction with CS/PT during the preparation of the nanoparticles. This strong electrostatic attraction between chitosan and pectin inhibited the release of NC from the CS/PT-complexed nanoparticles, as shown in Figure 2a. After incubating with SGF for 2 h, only 15% of NC was released from the NC-CS/PT-NPs. Subsequently, when incubated in pH 6.8 simulated intestine fluids for an additional 4 h, the release rate of NC increased to 21.9%. In contrast, when incubated in SCF, the NPs released 72.9% of the loaded NC within 14 h. These findings support previous reports and suggest that NC can be released from NC-CS/PT-NPs in response to the colon environment. The TEM images and size distribution of NC-CS/PT-NPs were tested under different simulated biological fluids, as shown in Figure 2b. The results confirmed the pH and microbial sensitivities of the delivery systems. In the lower GI site, chitosan is deprotonated, weakening the electrostatic attractions between chitosan and pectin compared to the upper GI. Additionally, the gut microflora can trigger the degradation of chitosan and pectin. The combination of gut microbiota-mediated degradation and weakened electrostatic attractions causes the collapse of NPs and the burst release of NC in the colon site. These findings suggest that CS/PT-NPs could be a promising carrier for colon delivery of NC. The unique characteristics of NC-CS/PT-NPs offer protection against degradation by intestinal enzymes and inhibit interactions between NC and the small intestinal mucosa, potentially enhancing therapeutic efficiency while reducing irritation in the upper GI.

NC-CS/PT-NPs Ameliorated Metabolic Disorders in the NAFLD Mice

Effects of NC-CS/PT-NPs on Mouse Liver Inflammatory Cells Histology

HFD can disrupt energy metabolism in NAFLD mice, leading to immune regulatory system dysfunction and subsequent liver inflammation. Liver stains, including H&E, Masson, ORO, and IHC, were used to assess the condition of the liver. The findings showed that HFD-fed mice exhibited hepatic steatosis, lobular inflammation, and noticeable hepatocyte bulbous formations (Figure 3). In comparison, the NC-CS/PT-NPs group displayed mild steatosis and reduced lipid droplets in the cytoplasm. Immunohistochemistry analysis of liver tissues from NAFLD mice also revealed the expression levels of Caspase-8, Nrf2, keap-1, and OH-1 (Figure 4). These results indicate that NC-CS/PT-NPs have the potential to alleviate NAFLD.

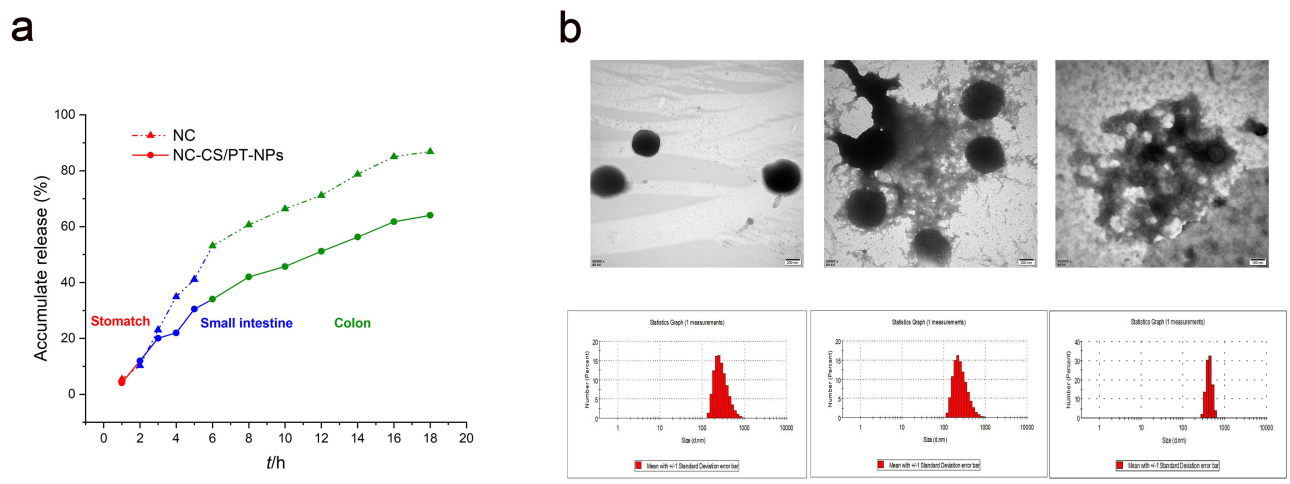

Figure 2 In Vitro Dissolution Study of NC-CS/PT-NPs. (**a**) Release curves of NC-CS/PT-NPs under different physiological pH conditions. (**b**) TEM of NC-CS/PT-NPs under different physiological pH conditions (200 nm).

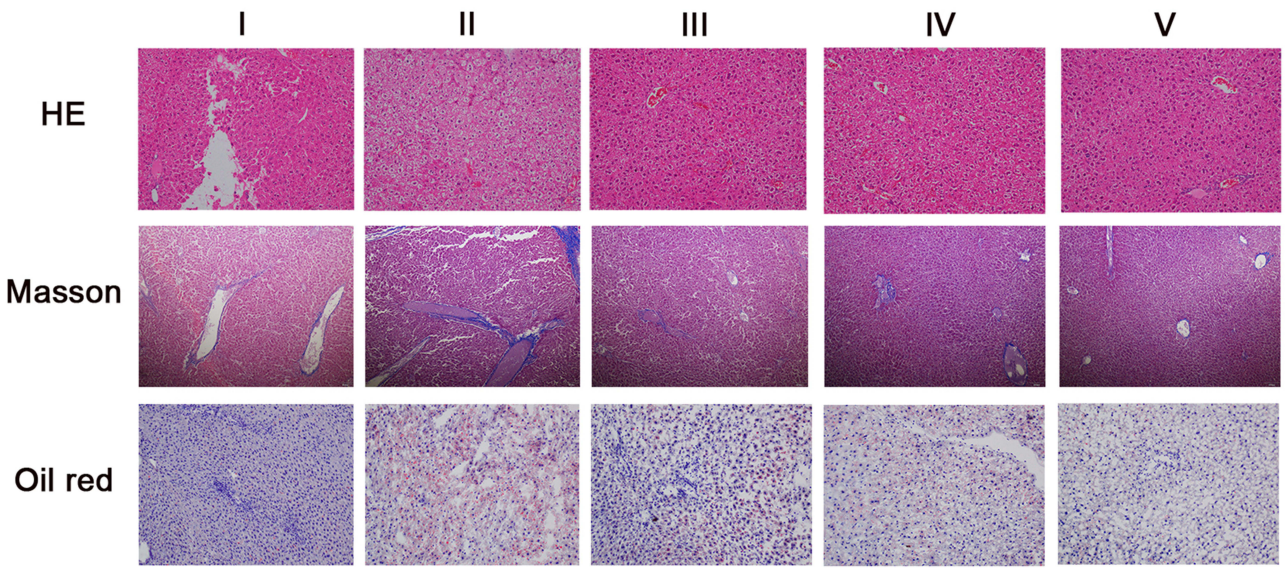

Figure 3 Effect of NC-CS/PT-NPs on pathological changes of liver tissue in NAFLD mice (HE staining, Masson staining, Oil red staining; ×200).
Notes: I: NCD group. II: HFD group. III: Positive Control group. IV: NC-treated group. V: NC-CS/PT-NPs treated group.

Effect of NC-CS/PT-NPs on Liver Index in Mice with NAFLD

The experimental results demonstrated that the liver index of mice in the HFD group was significantly higher compared to the NCD group (Figure 5a). However, the liver index of mice in all drug administration groups decreased, indicating that each drug administration group effectively reduced the liver index of mice induced by HFD-fed and inhibited liver enlargement and degeneration. Notably, the NC-CS/PT-NPs group exhibited a similar effect as the Positive group.

NC-CS/PT-NPs Improved Metabolic Parameters Associated with NAFLD

Compared to NCD group, HFD group for 20 weeks showed a significant increase in liver index ($p<0.05$), TC ($p<0.05$), TG ($p<0.05$), and LDL ($p<0.05$) (Figure 5b). However, when HFD-fed mice were administered NC-CS/PT-NPs (8 mg/kg/day NC) for 4 weeks, these disorders were significantly restored. Treatment with NC at the same dose also reduced liver index, TC, TG, and LDL, although to a lesser extent. The intervention with NC-CS/PT-NPs for 4 weeks effectively reversed these increases compared to the lack of treatment.

NC-CS/PT-NPs Improved Liver Inflammation Status in HDF-Fed Mice

Numerous studies have consistently shown a strong connection between obesity and metabolic disorders, particularly in relation to inflammatory responses. This association is further supported by the findings presented in Figure 5c, where the HFD group exhibited a significant increase in TNF-α, IL-β, IL-6, and MCP-1 levels compared to the NCD group, indicating notable impairment in liver function. However, after administering treatment with either NC or NC-CS/PT-NPs, the levels of TNF-α, IL-β, IL-6, and MCP-1 in mice fed a high-fat diet significantly decreased. It is worth noting that there were no significant differences observed between the two treatment groups.

NC-CS/PT-NPs Ameliorated Hepatic Steatosis and Liver Injury in HDF-Fed Mice

The serum levels of ALT and AST are two important biomarkers used to assess hepatic disease. As depicted in Figure 5d, the HFD-fed mice exhibited elevated levels of ALT and AST. However, treatment with NC-CS/PT-NPs significantly improved the ALT/AST levels compared to the HFD group. An increase in ALT/AST levels is commonly associated with the accumulation of liver fat, excluding alcohol consumption and viral hepatitis as possible causes of fatty liver. These findings suggest that the 4-week treatment with NC-CS/PT-NPs successfully protected the HFD-fed mice from hepatic injury.

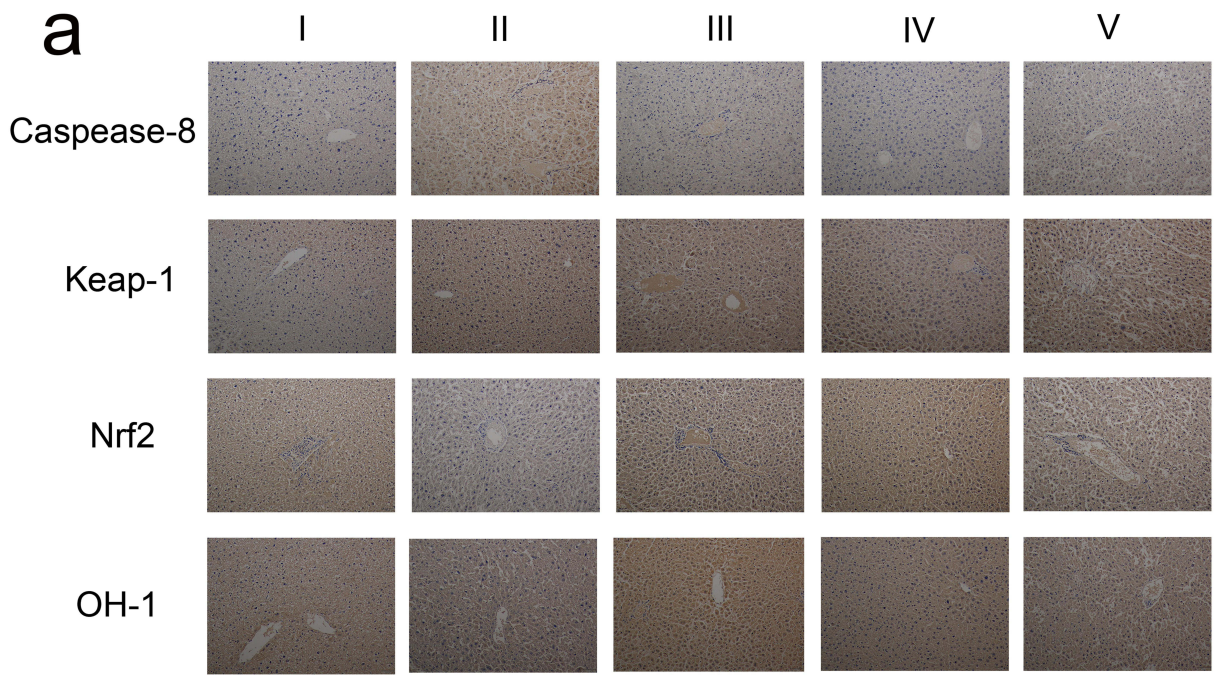

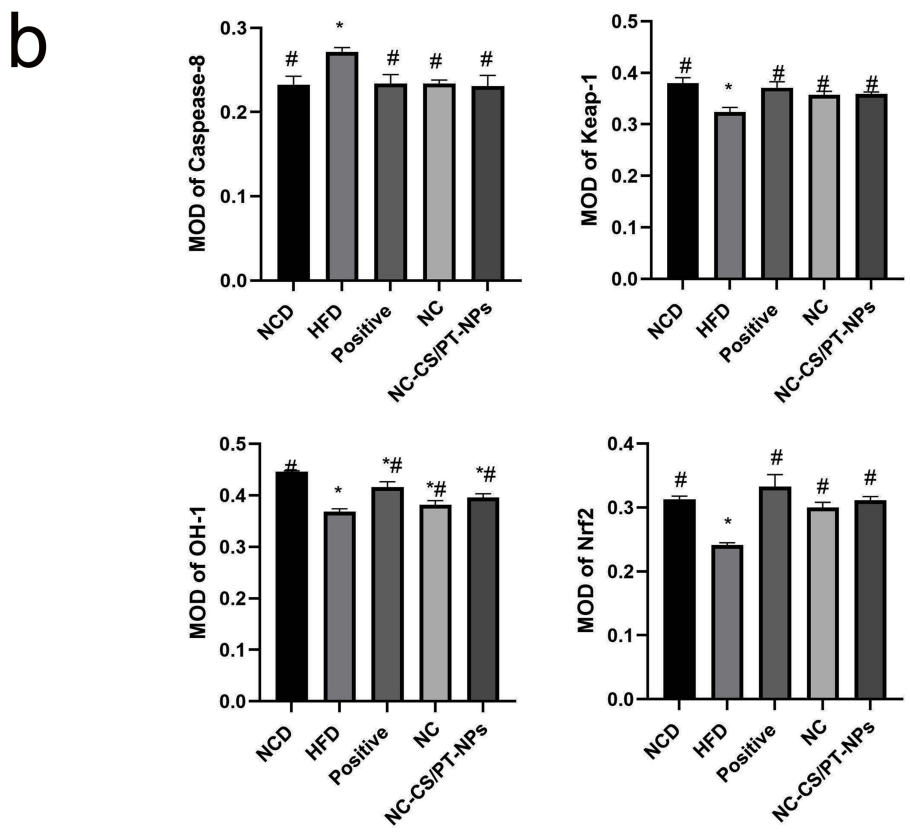

Figure 4 Effect of NC-CS/PT-NPs on pathological changes of liver tissue in NAFLD mice (IHC staining: ×200). (**a**) Immunohistochemical results of liver tissue in NAFLD mice. (**b**) Immunohistochemical examinations of Caspease-8, Keap-1, OH-1, Nrf2 in mice.

Notes: I: NCD group. II: HFD group. III: Positive Control group. IV: NC-treated group. V: NC-CS/PT-NPs treated group. Compared with NCD group, $^{*}p<0.05$; compared with HFD group, $^{\#}p<0.05$.

https://doi.org/10.2147/IJN.S452194 DovePress

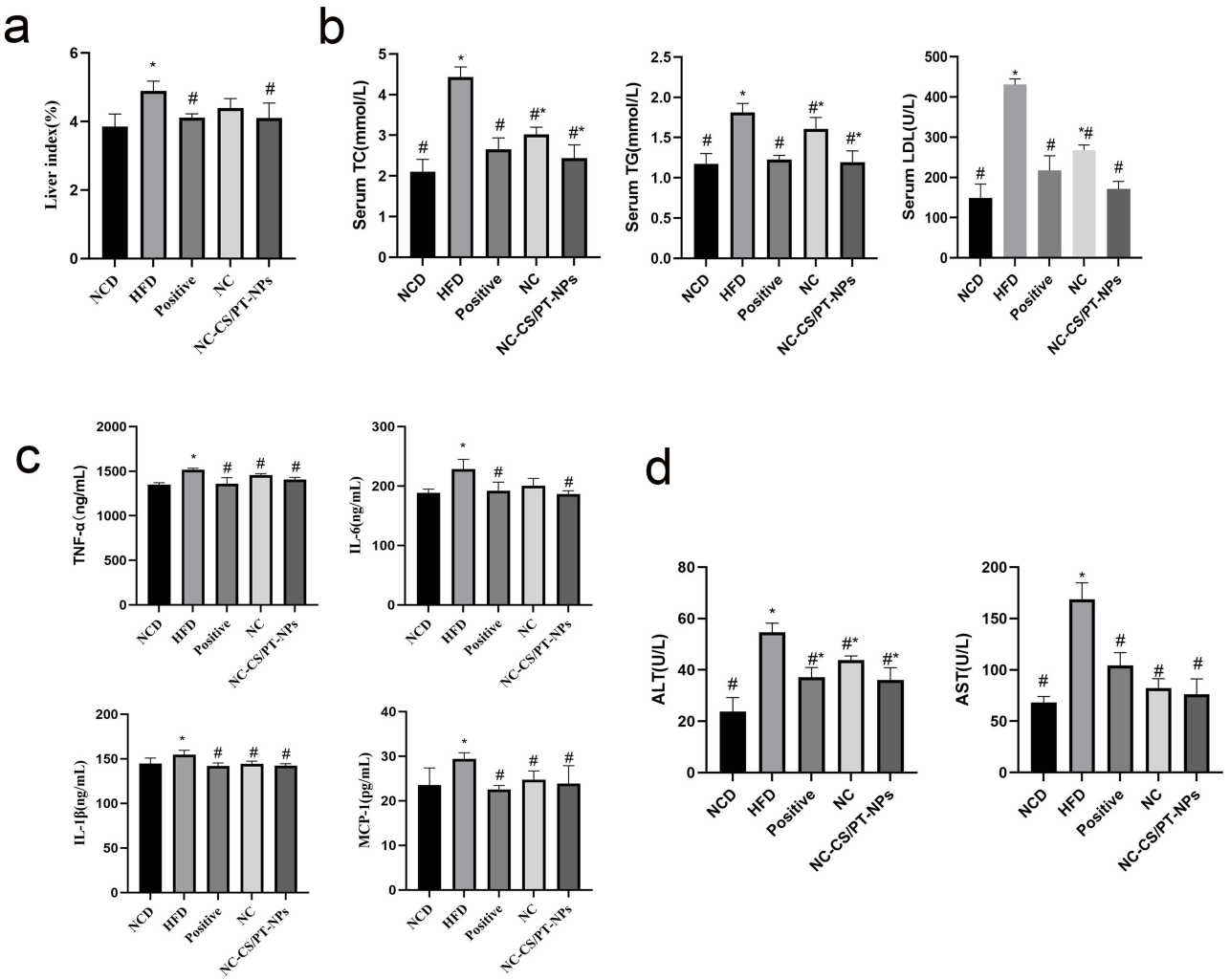

Figure 5 The Effect of NC-CS/PT-NPs on NAFLD Mice. (**a**) Liver Index of NAFLD Mice. (**b**) Serum TC, TG, LDL levels of mice in different groups. (**c**) TNF-α, IL-6, IL-β, MCP-1 levels in liver tissues of mice. (**d**) Serum ALT, AST levels of mice in different groups. Compared with NCD group, *$p<0.05$; compared with HFD group, $^{\#}p<0.05$.

NC-CS/PT-NPs Reduced Intestinal Inflammation in HFD-Fed Mice

Interactions between the gut microbiota play a crucial role in the development of inflammatory bowel disease. Several clinical trials have consistently shown that enhancing the diversity of the gut microbiota can effectively alleviate intestinal inflammation.[20] As illustrated in Figure 6, the intestinal mucosa of HFD-fed mice exhibited disturbances, including intestinal villous edema and a small amount of inflammatory cell infiltration, when compared to the NCD group. However, the colonic mucosal structure of mice in the Positive, NC-CS/PT-NPs groups showed significant

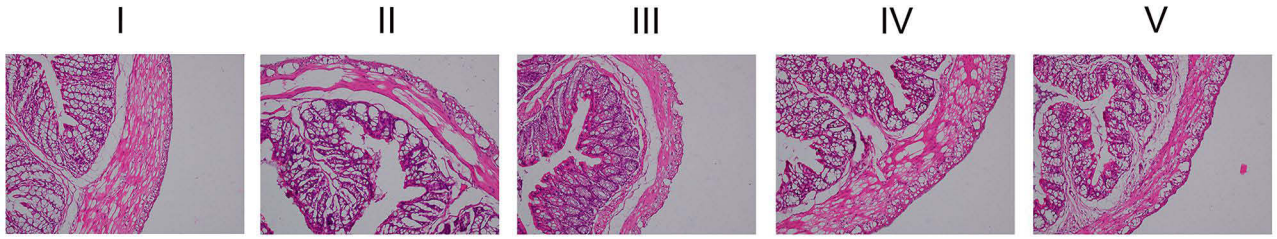

Figure 6 The Effect of NC-CS/PT-NPs on Colon Pathology in NAFLD Mice (HE staining; ×200).
Notes: I NCD group. II: HFD group. III: Positive Control group. IV: NC-treated group. V NC-CS/PT-NPs treated group.

improvement compared to the HFD group. These mice experienced reduced colonic tissue damage and alleviation of inflammatory cells.

The close association between obesity and metabolic disorders with inflammatory responses has been previously reported. In this study, we evaluated the levels of TNF-α, IL-β, IL-6, and MCP-1 in the colon using ELISA. Figure 7 illustrates that HFD-fed mice significantly induced inflammation compared to NCD-fed mice. The levels of TNF-α, IL-β, IL-6, and MCP-1 in the colon tissue were significantly higher in the HFD group than in the NCD group ($p<0.05$). The exposure of the positive group and the NC-CS/PT-NPs groups considerably inhibited this elevation ($p<0.05$). In the mice treated with NC, a less extensive decline was observed.

NC-CS/PT-NPs Effectively Restored the Microbiota Structure Variated by HFD

The output was obtained through Illumina high-throughput sequencing. A Venn diagram was used to visually represent the number of common and unique ASVs, illustrating sample similarity and overlap. As depicted in Figure 8a, the center of the diagram indicates the degree of overlap in species compositions among the five groups of environmental samples.

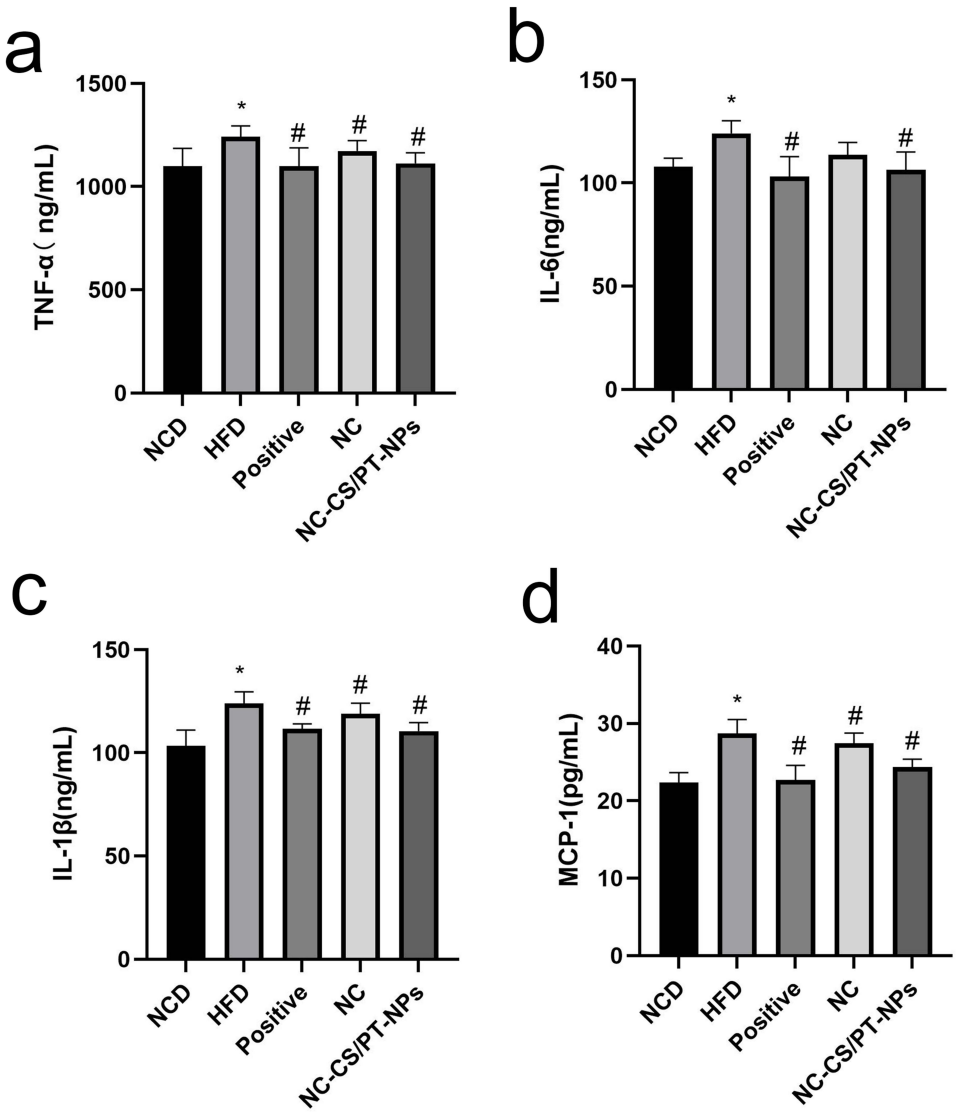

Figure 7 Effects of NC-CS/PT-NPs on pro-inflammatory factors in the colon of NAFLD mice. (**a**) TNF-α levels in colon tissues of mice. (**b**) IL-6 levels in colon tissues of mice. (**c**) IL-1β levels in colon tissues of mice. (**d**) MCP-1 levels in colon tissues of mice. Compared with NCD group, *$p<0.05$; compared with HFD group, #$p<0.05$.

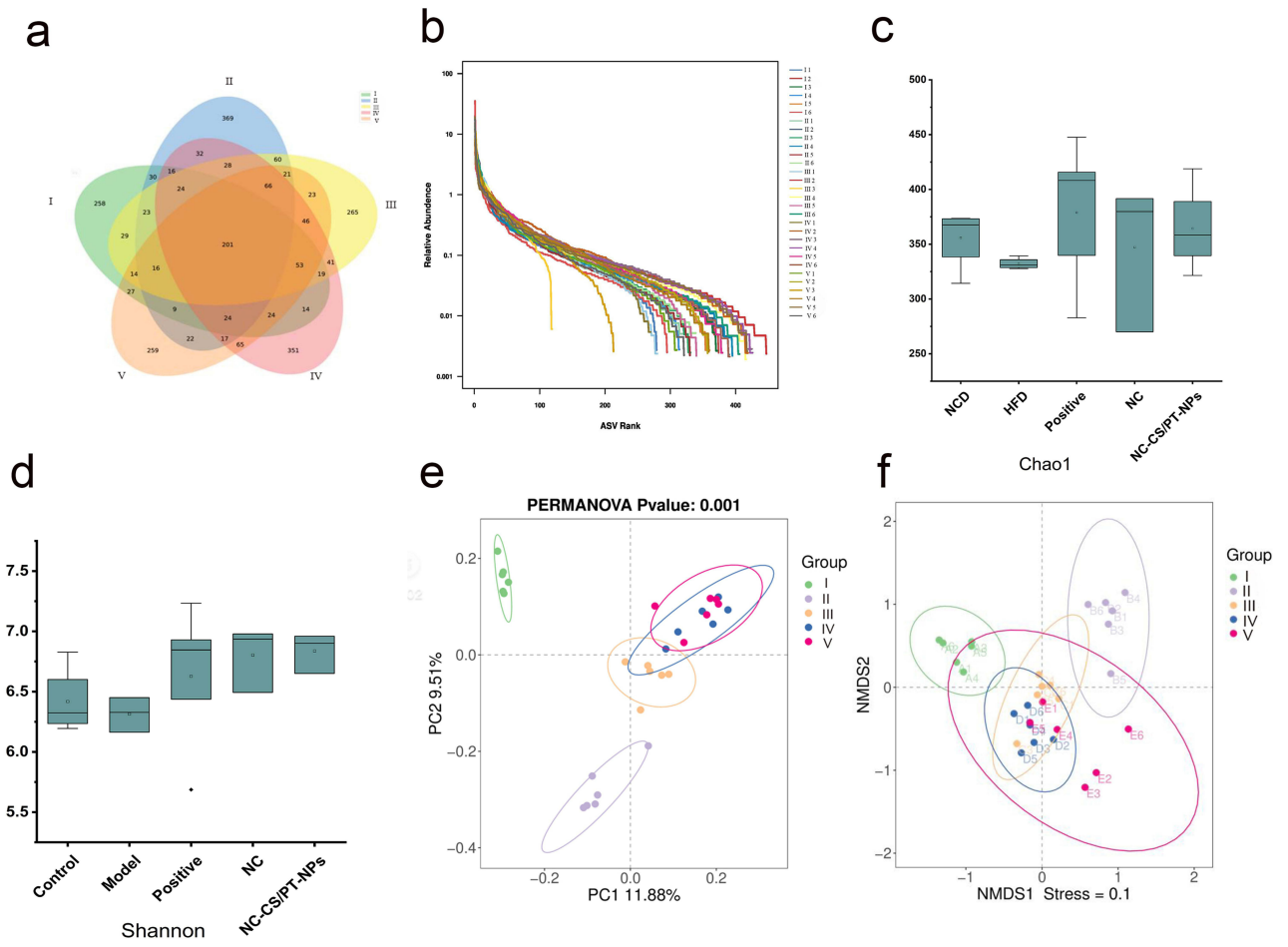

Figure 8 Analysis of gut microbiota diversity. (**a**) Venn diagram of each group. (**b**) OUT Rank Curve. (**c**) Chao1 index. (**d**) Shannon index. (**e**) PCA 2D analysis diagram. (**f**) NMDS Analysis Chart.
Notes: I NCD group. II: HFD group. III: Positive Control group. IV: NC-treated group. V NC-CS/PT-NPs treated group.

The inner part of the figure shows that 201 shared ASVs among the five mice groups, while group shared 258,369,265,351 and 259 ASVs with group I, II, III, IV and V, respectively.

Rank Abundance refers to the richness and uniformity of species in a sample. A wider curve indicates a richer species composition, while a flatter curve suggests a more homogeneous composition. In Figure 8b, it can be observed that the HFD group showed a decrease in abundance and homogeneity compared to the NCD group. However, after treatment with NC-CS/PT-NPs, both abundance and homogeneity increased.

Alpha diversity refers to the diversity within a specific area or ecosystem. Commonly used metrics, such as Chao 1 and Shannon indices, are used to measure species diversity and gather additional information through observation. The results indicate that there was no significant difference in the richness of gut microbiota between the NCD group and HFD group (Chao1 index, Figure 8c), suggesting that HFD feeding did not have a dramatic impact on the bacterial richness and diversity in NAFLD mice. However, the Shannon index in the HFD group was lower compared to the NCD group, indicating a decrease in bacterial diversity in NAFLD mice (Figure 8d). Although the NC group and NC-CS/PT-NPs group exhibited higher gut community diversity compared to the HFD group, the difference was not statistically significant. Overall, the analysis of alpha diversity showed a decrease in the richness and diversity of gut microbes in NAFLD mice, and the intervention of NC-CS/PT-NPs did not affect the bacterial stability of the intestinal ecosystem.

Weighted Unifrac principal component analysis (PCA) and principal coordinate analysis (PCoA) revealed distinct compositional differences in gut microbiota between the high fat diet (HFD) and normal chow diet (NCD) groups (Figure 8e). The first principal component factor of PCA accounted for 6.5% of the variation, while the second principal

component factor accounted for 5.73%. Similarly, the first principal component (PC1) factor of PCoA explained 11.88% of the variation, and the second principal component (PC2) factor explained 9.51%. The analysis revealed that the positive group, NC group and NC-CS/PT-NPs group partially corrected the variation induced by HFD along PC2, but did not have a significant effect on the movement of PC1. On the other hand, the samples from the HFD group and NC group were more dispersed, indicating significant differences in the gut microbiota between these two groups. Notably, NC treatment (NC group or NC-CS/PT-NPs group) partially restored the microbiota composition towards that of the NCD group, which had been disrupted by the HFD group. These findings suggest that NC treatment has the potential to improve the Beta diversity of gut microbiota.

Through inter-group comparative analysis of species diversity among different microbial communities (Figure 8f), we explored similarities or differences in community composition among samples from different subgroups. NMDS analysis revealed distinct clustering patterns of microbiota composition within each group, with a stress value commonly considered to be less than 0.2, indicating certain explanatory significance for the results obtained in this study (stress=0.099). It was observed that the intervention of HFD group mice and each administration group significantly influenced the composition of intestinal microbiome. The intestinal microbiome of HED group exhibited complete separation from that of NCD group, while the distance between each administration group and NCD group was much smaller compared to that between HFD group and NCD group, suggesting that the administration groups regulated changes in intestinal microbiome structure.

According to the distance matrix obtained using various distance algorithms, the hierarchical clustering of the matrix clearly reveals the inter-sample distances (Figure 9). The blue color represents closer distances and higher similarity between samples, while red indicates greater distances. The heat map facilitates sample clustering, and the clustering tree provides insights into the distance relationships among samples. In terms of Euclidean_distance and Weighted_unifrac_distance, the

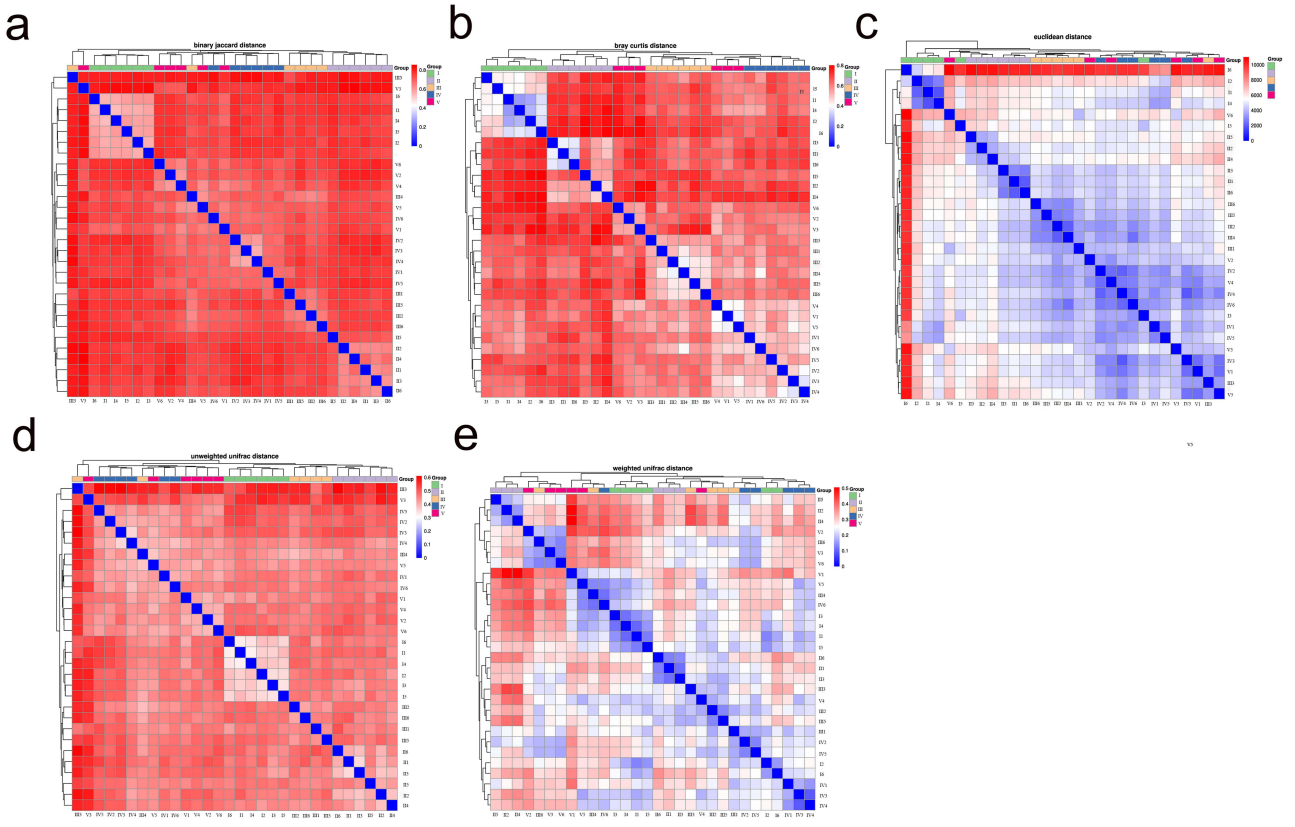

Figure 9 Sample distance heat map. (**a**) Binary_jaccard_distance. (**b**) Bray_curtis_distance. (**c**) Euclidean_distance. (**d**) Unweighted_unifrac_distance. (**e**) Weighted_unifrac_distance.
Notes: I NCD group. II: HFD group. III: Positive Control group. IV: NC-treated group. V NC-CS/PT-NPs treated group.

reproducibility of each group is higher. The difference between NCD group and HFD group was large, while the difference between the treatment groups and NCD group was small.

The results of the gut microbiota abundance analysis revealed the top 10 phyla with relative abundance in each group, as shown in Figure 10a. In comparison to the NCD group, the HFD group exhibited a significant decrease in the abundance of *Bacteroidetes*, while *Desulfobacterota* and *Proteobacteria* showed a remarkable increase. The elevated prevalence of the bacterial phylum *Proteobacteria* indicates an unstable microbial community (dysbiosis) and a potential diagnostic criterion for disease.[21] Following treatment with NC (NC group and NC-CS/PT-NPs group), the abundance of *Bacteroidetes* gradually increased, whereas that of *Desulfobacterota* and *Proteobacteria* decreased gradually. To visually represent this change, we have presented the proportion of *Firmicutes* to *Bacteroidetes* in Figure 10f. Notably, the F/B ratio exhibited a significant statistical difference between the NCD group and the HFD group, indicating a decrease in *Bacteroides* and an increase in *Firmicutes* in the HFD group. Compared to the HFD group, the F/B ratio of the NC-CS /PT-NPs group showed a significant decrease, while the F/B ratio did not change significantly in the NC group. The abundance of *Desulfobacterota, Campilobacterota*, and *Deferribacteres* in the HFD group exhibited a significant increase compared to the NCD group (Figure 10g). After treatment, the relative abundance of each group decreased significantly, returning to levels similar to those observed in the NCD group. Compared to the NC group, the relative abundance of the NC-CS/PT-NPs group was more similar to that of the Positive group and NCD group, suggesting that NC-CS/PT-NPs have a better ability to regulate intestinal colony homeostasis. The microbial profiles at the class level showed a similar pattern as previous findings (Figure 10b and h). In comparison to the mice in the NCD group, a significant change was observed in the relative abundance of *Campylobacteria* and *Deferribacteres*, which increased in HFD-induced mice. Additionally, there was a noticeable decrease in the relative abundance of these three groups in the intestinal flora of mice in the treatment group. At the Order level, there was a significant increase and difference in the relative abundance of *Oscillospirales* and *Campylobacterales* in the HED group compared to the Control group (Figure 10c and i). After treatment, both groups experienced a reduction in relative abundance, although to varying degrees. Additionally, the NC-CS/PT-NPs group showed a more effective ability to regulate the intestinal flora of mice compared to the NC group. These findings suggest that NC-CS/PT-NPs had a significant impact on restoring the abundance of *Bacteroidetes* and *Desulfobacterota*. At the family level, administration of NC-CS/PT-NPs greatly increased the levels of *Muribaculaceae* and *Helicobacteraceae* in diet-induced obese mice, which were induced by HFD. On the other hand, it attenuated the abundance of *Ruminococcaceae* (Figure 10d and j). At the genus level, after NC-CS/PT-NPs treatment, *Alloprevotella* increased, *[Eubaclerium]_ coproslanoligenes_ group, Lactobacillaceae, Muribaculaceae, Ruminococcaceae* and *Helicobacteraceae* were significantly different in the five groups (Figure 10e and k).

According to the clustering heat map analysis results, NC-CS/PT-NPs treatment showed a significant restoration in the abundance of several key bacteria such as *Acidobacteriota, Anaeroplasma, Bacteroidetes* that were disrupted by HFD (Figure 11), which might affect the homeostasis of the gut microenvironment and is closely associated with metabolic disorders. In addition to reducing the abundance of *Verrucomicrobiota*, which is known to be associated with weight control,[22] the NC-CS/PT-NPs also attenuated the abundance of *Erysipelotrichaceae, Firmicutes, Izemoplasmatales* and *Desulfovibrionia*. It is worth noting that *Firmicutes* and *Colidextribacter* are considered to be SCFA producers.[23] On the other hand, the increased abundance of *Desulfovibrionia* is known to promote the formation of endotoxemia and contribute to the pathogenesis of NAFLD.[24,25]

The linear discriminant analysis (LDA) effect size branching plot revealed significant differences in taxa between various treatments (Wilcoxon rank sum test, $p< 0.05$) (Figure 12a and b). The size of the circle in the branching diagram was proportional to the abundance of bacteria, representing phyla, class, order, family, and genus from the inner to the outer circle. The LDA histogram demonstrated biomarkers with statistical differences among all groups, with only the absolute value of LDA greater than 3.5 considered significant. In the NCD group, significant roles were played by bacterial groups such as *Butyrivibrio, Muribaculum, Marinifilaceae, Odoribacter, Anaeroplasma, Acholeplasmatales, Acholeplasmataceae*, among others. The HFD group included bacterial groups such as *Oscillospirales, Desulfobacterota, Desulfovibrionales, Desulfovibrionia, Desulfovibrionaceae, uncultured, Paraprevotella, Rikenellaceae, Proteobacteria, Eubacterium siraeum group, Alistipes, Rikenellace eael R 9 gut group, Clostridia vadinBB60 group, Clostridiavad inBB60 group, Clostridia vadinBB60 group, Alphaproteobacteria*, among others. Following the administration of the drug, the group receiving the

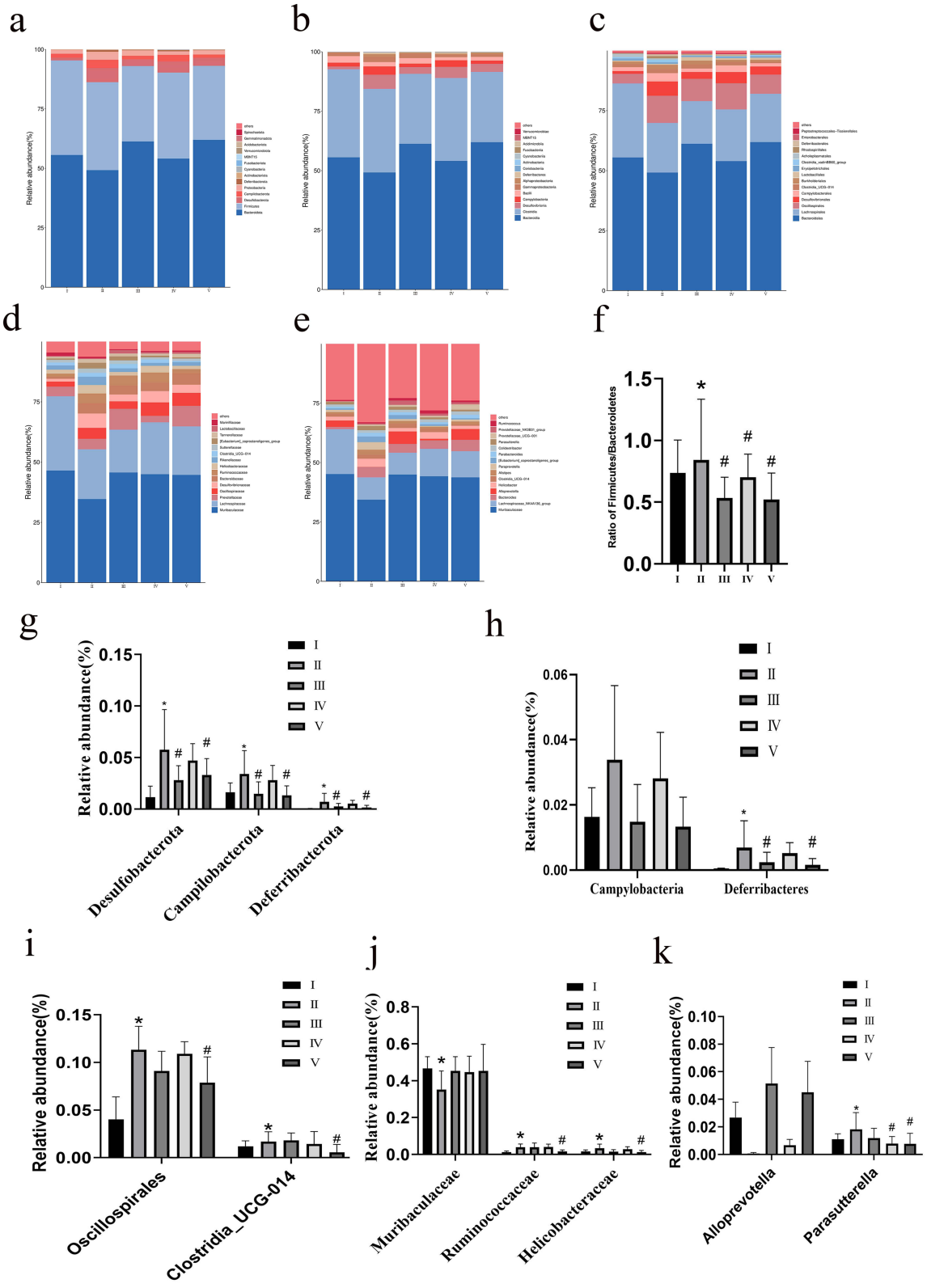

Figure 10 The effect of NC-CS/PT-NPs on gut microbiome composition of mice induced by HFD in different taxa. (**a**) Phylum. (**b**) Class. (**c**) Order. (**d**) Family. (**e**) Genus. (**f**) The ratio of *Firmicutes* /*Bacteroidota*. (**g**) Relative abundance of Phylum. (**h**) Relative abundance of Class. (**i**) Relative abundance of Order. (**j**) Relative abundance of Family. (**k**) Relative abundance of Genus. Compared with NCD group, *$p<0.05$; compared with HFD group, $^{\#}p<0.05$.

Notes: I NCD group. II: HFD group. III: Positive Control group. IV: NC-treated group. V NC-CS/PT-NPs treated group.

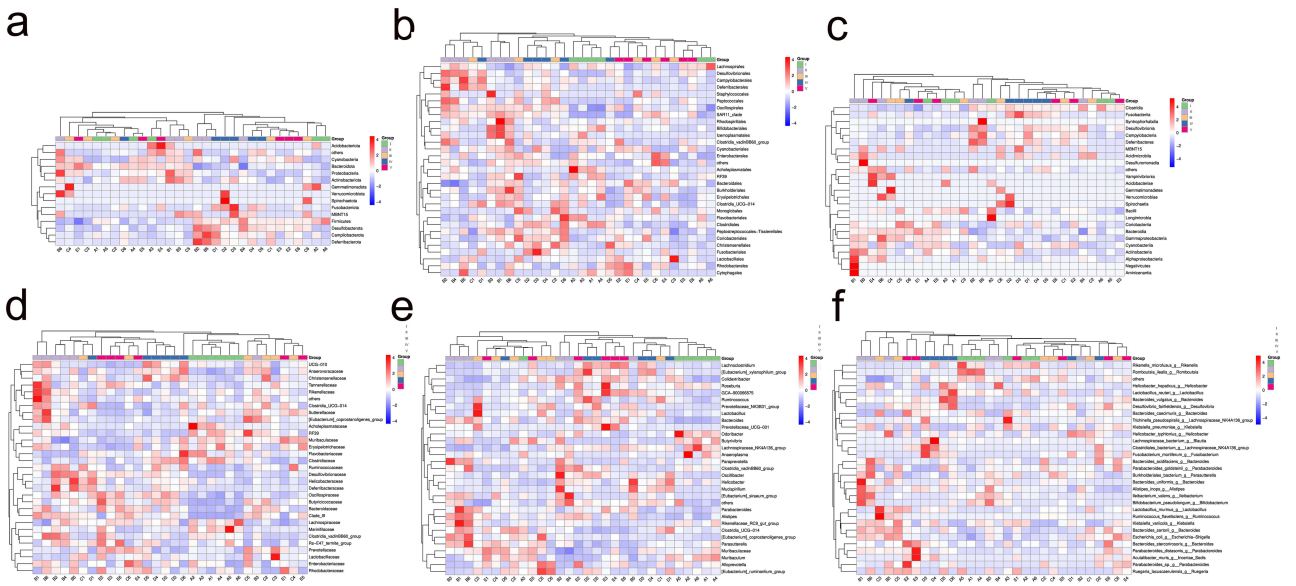

Figure 11 The effect of NC-CS/PT-NPs on intestinal microbiome composition of mice induced by HFD by clustering heat map. (**a**) Phylum. (**b**) Class. (**c**) Order. (**d**) Family. (**e**) Genus. (**f**) Species.
Notes: I NCD group. II: HFD group. III: Positive Control group. IV: NC-treated group. V NC-CS/PT-NPs treated group.

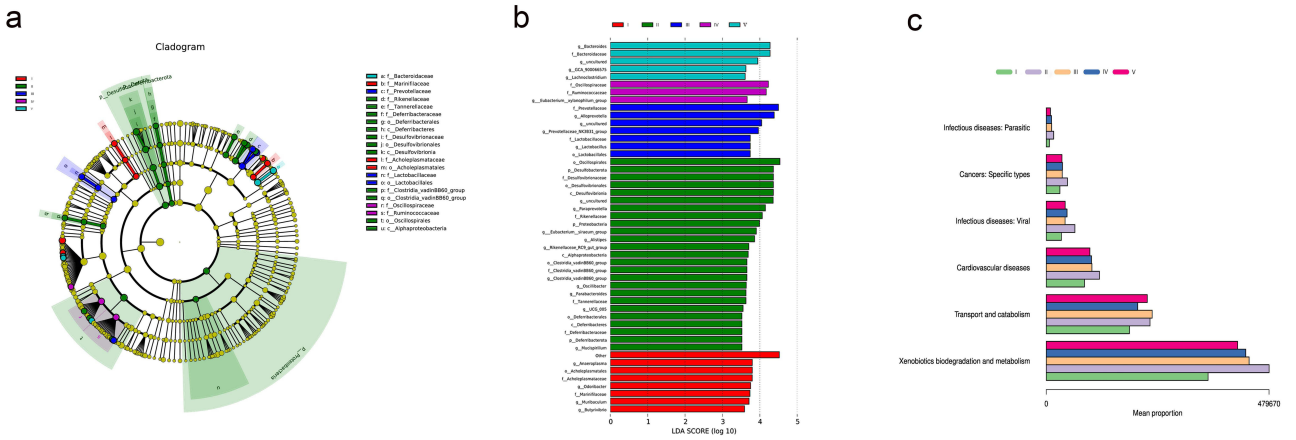

Figure 12 Composition of different species in different groups of biomes. (**a**) Cladogram. (**b**) LDA SCORE. (**c**) KEGG.
Notes: I NCD group. II: HFD group. III: Positive Control group. IV: NC-treated group. V NC-CS/PT-NPs treated group.

drug showed an increase in the presence of *Prevotellaceae, Alloprevotella*, uncultured bacteria, *Prevotellaceae NK3B31 group, Lactobacillaceae, Lactobacillus*, and other bacterial groups such as *Lactobacillales*. In contrast, the NC group had *Oscillospiraceae, Ruminococcaceae*, and the *Eubacterium_xylanophilum group*. The group receiving the drug in combination with NC-CS/PT-NPs group exhibited the emergence of *Bacteroides, Bacteroidaceae, uncultured bacteria (GCA900066575), Lachnoclostridium*, and other bacterial groups. To gain insight into the potential function of colonic microbiota, we conducted KEGG analysis and identified the top 6 KEGG pathways among the five groups (Figure 12c). In the HFD group, the gut microbiotas were primarily associated with Infections diseases: Parasitic and Viral, Cancers: Specific types, Cardiovascular diseases, and Xenobiotics biodegradation and metabolism. In the Positive group, the gut microbiotas were mainly involved in Transport and catabolism, as well as Xenobiotics biodegradation and metabolism. In the NC group, the gut microbiotas were primarily associated with Infections diseases: Viral, Cardiovascular diseases, and Xenobiotics biodegradation and metabolism. Lastly, in the NC-CS/PT-NPs group, the gut microbiotas were primarily involved in Transport and catabolism.

Discussion

Hepatic steatosis is the early stage of NAFLD, and it can progress to non-alcoholic steatohepatitis (NASH), liver fibrosis, cirrhosis and eventually hepatocellular carcinoma.[26] The liver is exposed to the gut microbiota and its metabolites through the gut-liver axis, which connects the gut to the liver. Several studies have demonstrated that traditional Chinese medicine can modulate and treat diseases through the regulation of intestinal flora and the intestinal barrier.[27,28] This study aimed to investigate the protective effect of colon-targeted nanomaterials NC-CS/PT-NPs on HFD-induced NAFLD in mice, partially mediated by the modulation of intestinal.

CS, a partially deacetylated chitin, has been widely utilized as a polymeric drug carrier in drug delivery applications. This natural polymer possesses numerous attractive features, including biocompatibility, biodegradability, low toxicity, and pH sensitivity.[29] PT is a natural high molecular acid polysaccharide polymer extracted from plant tissue. It is often used as a carrier material for oral colonic drugs due to its favorable characteristics, such as accurate colon localization, controlled and slow release, and minimal impact from gut pH. Several studies have indicated that chitosan and pectin can function as prebiotics in the treatment of high blood lipids and obesity by modulating the gut microbiota.[30,31] One major drawback of pectin-based delivery systems is the solubility and swelling properties of pectin in aqueous media. This can result in the premature release of the bioactive component while passing through the upper gastrointestinal tract, before reaching the colon. To overcome this issue, researchers have explored various strategies. These include blending pectin with metal salts, compounding it with other polymers, and introducing hydrophobic groups. These approaches effectively reduce the water solubility and swelling properties of pectin as a carrier for oral colon-targeted drug delivery systems. By doing so, they prevent the premature release of the bioactive component during transit through the upper gastrointestinal tract, ensuring its delivery to the colon.[32] Chitosan exhibits a positive charge at low pH levels, leading to its spontaneous association with negatively charged pectin in solution. This association occurs through an ionic interaction between the ionized amino group of chitosan and the ionized carboxyl group of pectin, resulting in the formation of polyelectrolyte complexes.[33] In this study, chitosan and pectin were used as carrier materials for oral administration. A polyelectrolyte composite nanoparticle was designed to have a specific response to the physiological environment of the colon. The drug NC, which protects the liver, was encapsulated in these nanoparticles. Upon oral administration, the strong electrostatic attractions between pectin and chitosan resulted in a slower release of NC in the gastrointestinal environment, facilitating its smooth delivery to the colon. In the microbiota-rich segment of the colon, the combination of the higher physiological pH and the presence of intestinal microbiota triggered the degradation of chitosan and pectin, leading to the collapse of the nanoparticles. This collapse exposed a significant amount of nitidine chloride to the gut microbiota.

Alterations in gut microbiota have been described in a wide variety of diseases such as cirrhosis, Parkinson diseases and autism. Compiling evidence indicates that the disruption of dietary-induced gut microbiota homeostasis is closely related to the development of obesity and metabolic-related diseases. NC-CS/PT-NPs might play a role in the treatment of obesity and related metabolic disorders by regulating the disturbance of intestinal microbial flora.[19] The histopathological results demonstrated that the administration of NC-CS/PT-NPs significantly enhanced the disappearance of crypts and reduced inflammatory cell infiltration. In addition, we examined the potential impact of NC-CS/PT-NPs on NAFLD by modulating the composition of the gut microbiota. Our findings demonstrate that supplementation with NC-CS/PT-NPs effectively mitigated liver damage caused by HFD-fed, resulting in increased body weight and reduced liver weight in mice. NAFLD is commonly linked to metabolic dyslipidemia, which is characterized by elevated levels of TG, TC, and LDH. ALT and AST are considered the most sensitive indicators of hepatotoxicity and provide direct insight into the progression of NAFLD. The low levels of these indicators also indicate the therapeutic effect of NC-CS/PT-NPs; this is consistent with the results in coffee peel extracts treated mice and rats with NAFLD treated with total flavonoids of Qu Zhi Ke.[34,35] The production and release of inflammation cytokines, such as TNF-α, IL-1β, and IL-6, have become important factors affecting the progression and prognosis of NAFLD. Previous studies have reported that the IL-1β pathway mediates steatosis, inflammation, and fibrosis, and interfering with IL-1β may play a significant role in the treatment of non-alcoholic liver injury.[36] The results of this study showed that the supplementation of NC-CS/PT-NPs in mice led to lower levels of TNF-α, IL-1β, and IL-6. This suggests that NC-CS/PT-NPs have the potential to decrease inflammatory reactions in the liver. Previous research has confirmed that patients with NAFLD have higher levels of

TNF-α and soluble TNFR1, which are positively correlated with the severity of the disease.[37] Therefore, these findings indicate that NC-CS/PT-NPs can help alleviate hepatic injury caused by a high-fat diet by reducing liver inflammation.

The role of gut microbiota in metabolic diseases, such as obesity and NAFLD, has been extensively studied.[38–40] Studies have shown that the composition of *Bacteroidetes, Firmicutes*, and *Proteobacteria* in the gut is significantly altered in mice fed high-fat diets.[41,42] In an animal model of HFD-induced metabolic disorder, *Firmicutes* was found to be the most predominant phylum, followed by *Bacteroidetes*.[40] Furthermore, patients with NAFLD were observed to have a decrease in Gram-positive *Firmicutes* and an increase in Gram-negative *Proteobacteria* compared to healthy individuals.[9,43] The results of our study revealed that HFD-fed mice showed a significant increase in the relative abundance of *Firmicutes* and a higher *Firmicutes*-to-*Bacteroidetes* ratio compared to chow-fed mice. Treatment with NC-CS/PT-NPs increased the *Firmicutes*-to-*Bacteroidetes* ratio. Additionally, NC-CS/PT-NPs reduced the abundance of *Desulfobacterota, Campylobacterota*, and *Deferribacteres*. Previous studies have reported that patients with abnormal levels of ALT or AST have higher levels of *Firmicutes* and lower levels of *Bacteroidetes*.[44] At the class level, *Campylobacter*, a gram-negative bacterium, is not commonly found in the gut microbiota of healthy individuals but is more prevalent in the oral and intestinal microbiota of patients with Inflammatory Bowel Disease (IBD).[45] The *Campylobacter* zot808T gene encodes Zot, a toxin that disrupts the integrity of the intestinal barrier and induces an inflammatory response in host epithelial cells.[46] At the Order level, administration of NC-CS/PT-NPs significantly reduced the HFD-induced increase in *Oscillospirales* and *Campylobacterales*. *Oscillospirales* has been found to be positively associated with leanness or low body mass index in both children and adults.[47] At the family level, treatment with NC-CS/PT-NPs restored the abundance of several bacterial families that have been linked to short-term mortality, including *Lactobacillaceae, Muribaculaceae, Ruminococcaceae*, and *Helicobacteraceae*.[48] At the genus level, the HFD group significantly decreased the relative abundance of *Alloprevotella* in rats, while drug administration significantly increased its relative abundance. Comparatively, the NC-CS/PT-NPs group exhibited a more pronounced effect compared to the NC group. *Alloprevotella* has the ability to ferment complex carbohydrates into short-chain fatty acids (SCFAs), which in turn enhance insulin resistance and improve glucose metabolism disorders.[49]

Previous studies have demonstrated that the intestinal flora plays a crucial role in influencing the microbiota-liver axis, thereby regulating metabolic diseases such as NAFLD, diabetes, and obesity.[41,50,51] Our research findings further support this notion by showing that HFD-induced can disrupt the structure and abundance of the intestinal microbiota, leading to increased systemic inflammation. However, we discovered that the administration of colon-specific gut microbiota-targeting NC-CS/PT-NPs can effectively alleviate NAFLD by modulating intestinal dysbiosis. Notably, the therapeutic efficacy of NC-CS/PT-NPs surpasses that of NC alone due to its enhanced interaction with the gut microbiota.

In this study, we have developed and designed a dual stimulus-responsive Nano-carrier system (NC-CS/PT-NPs) that is responsive to pH and intestinal microbiota. The purpose of this system is to enhance the targeting of NC to the colon. After administering NC-CS/PT-NPs, we observed a reduction in NAFLD induced by HFD-fed in mice. Additionally, there was a decrease in liver tissue and intestinal inflammation. This is the first formulation that specifically targets NC to modulate the gut microbiota through the colon for disease treatment. Further investigation is warranted to explore the potential of this system.

Conclusion

The NC-CS/PT-NPs were synthesized using the ion gel method and subjected to comprehensive characterization. NC-CS /PT-NP is a colon-targeted nanoparticle that mitigated NAFLD in mice HFD-induced by modulating intestinal microbiome disturbances. Therefore, NC-CS/PT-NPs hold promise as a drug delivery system that facilitates the clinical application of NC.

Acknowledgments

Thank you to everyone who has provided us with assistance during our experiments and writing papers. It is our great pleasure to acknowledge the help we have received from our supervisors, Professor Ye, who has provided us with valuable suggestions during our academic studies.

Funding

This study was supported by grants from National Natural Science Foundation of China (No. 82360818), the Natural Science Foundation of Guangxi Province (No.2022GXNSFDA035063, 2023GXNSFAA026366), First-class discipline innovation-driven talent program of Guangxi Medical University, Guangxi Medical University Training Program for Distinguished Young Scholars.

Disclosure

There are no competing financial interests or personal relationships that could influence the work reported in this study.

References

1. Mouries J, Brescia P, Silvestri A, et al. Microbiota-driven gut vascular barrier disruption is a prerequisite for non-alcoholic steatohepatitis development. *J Hepatol*. 2019;71(6):1216–1228. doi:10.1016/j.jhep.2019.08.005
2. Miele L, Valenza V, La Torre G, et al. Increased intestinal permeability and tight junction alterations in nonalcoholic fatty liver disease. *Hepatology*. 2009;49(6):1877–1887. doi:10.1002/hep.22848
3. Murata Y, Mizuno S, Kato H, et al. Nonalcoholic steatohepatitis (NASH) after pancreaticoduodenectomy: association of pancreatic exocrine deficiency and infection. *Clin J Gastroenterol*. 2011;4(4):242–248. doi:10.1007/s12328-011-0226-9
4. Le MH, Yeo YH, Li X, et al. 2019 global NAFLD prevalence: a systematic review and meta-analysis. *Clin Gastroenterol Hepatol*. 2022;20 (12):2809–2817.e2828. doi:10.1016/j.cgh.2021.12.002
5. Zhou J, Zhou F, Wang W, et al. Epidemiological Features of NAFLD From 1999 to 2018 in China. *Hepatology*. 2020;71(5):1851–1864. doi:10.1002/hep.31150
6. Sodum N, Kumar G, Bojja SL, Kumar N, Rao CM. Epigenetics in NAFLD/NASH: targets and therapy. *Pharmacol Res*. 2021;167:105484. doi:10.1016/j.phrs.2021.105484
7. Rong L, Zou J, Ran W, et al. Advancements in the treatment of non-alcoholic fatty liver disease (NAFLD). *Front Endocrinol*. 2022;13:1087260. doi:10.3389/fendo.2022.1087260
8. Boursier J, Mueller O, Barret M, et al. The severity of nonalcoholic fatty liver disease is associated with gut dysbiosis and shift in the metabolic function of the gut microbiota. *Hepatology*. 2016;63(3):764–775. doi:10.1002/hep.28356
9. Loomba R, Seguritan V, Li W, et al. Gut microbiome-based metagenomic signature for non-invasive detection of advanced fibrosis in human nonalcoholic fatty liver disease. *Cell Metab*. 2017;25(5):1054–1062.e1055. doi:10.1016/j.cmet.2017.04.001
10. Alferink LJM, Radjabzadeh D, Erler NS, et al. Microbiomics, metabolomics, predicted metagenomics, and hepatic steatosis in a population-based study of 1355 adults. *Hepatology*. 2021;73(3):968–982. doi:10.1002/hep.31417
11. Hong Y, Xu WQ, Feng J, et al. Nitidine chloride induces cardiac hypertrophy in mice by targeting autophagy-related 4B cysteine peptidase. *Acta Pharmacol Sin*. 2023;44(3):561–572. doi:10.1038/s41401-022-00968-6
12. Chen YW. *Pharmacokinetic and Pharmacodynamic Study of Nitidine Chloride Solid Lipid Nanoparticles*. Guangxi Medical University; 2010.
13. Zhao S, Jiang L, Mu YN, et al. Study on intestinal absorption of nitidine chloride. *Chin Med Mod Dist Educ China*. 2018;16(10):96–97+105.
14. Mitchell MJ, Billingsley MM, Haley RM, Wechsler ME, Peppas NA, Langer R. Engineering precision nanoparticles for drug delivery. *Nat Rev Drug Discov*. 2021;20(2):101–124. doi:10.1038/s41573-020-0090-8
15. Hoshyar N, Gray S, Han H, Bao G. The effect of nanoparticle size on in vivo pharmacokinetics and cellular interaction. *Nanomedicine*. 2016;11 (6):673–692. doi:10.2217/nnm.16.5
16. Wu P, Han J, Gong Y, Liu C, Yu H, Xie N. Nanoparticle-based drug delivery systems targeting tumor microenvironment for cancer immunotherapy resistance: current advances and applications. *Pharmaceutics*. 2022;14(10):1990. doi:10.3390/pharmaceutics14101990
17. Li S, Zhang H, Chen K, et al. Application of chitosan/alginate nanoparticle in oral drug delivery systems: prospects and challenges. *Drug Delivery*. 2022;29(1):1142–1149. doi:10.1080/10717544.2022.2058646
18. Chen S, Zhu H, Luo Y. Chitosan-based oral colon-specific delivery systems for polyphenols: recent advances and emerging trends. *J Mat Chem B*. 2022;10(37):7328–7348. doi:10.1039/D2TB00874B
19. Guo -H-H, Ma C, Zheng W-S, et al. Dual-stimuli-responsive gut microbiota-targeting berberine-CS/PT-NPs improved metabolic status in obese hamsters. *Adv Funct Mater*. 2020;30(13):1910337. doi:10.1002/adfm.201910337
20. Li Y, Zhao D, Qian M, et al. Amlodipine, an anti-hypertensive drug, alleviates non-alcoholic fatty liver disease by modulating gut microbiota. *Br J Pharmacol*. 2022;179(9):2054–2077. doi:10.1111/bph.15768
21. Albillos A, de Gottardi A, Rescigno M. The gut-liver axis in liver disease: pathophysiological basis for therapy. *J Hepatol*. 2020;72(3):558–577. doi:10.1016/j.jhep.2019.10.003
22. Zhang Y, Yang L, Zhao N, et al. Soluble polysaccharide derived from laminaria japonica attenuates obesity-related nonalcoholic fatty liver disease associated with gut microbiota regulation. *Mar Drugs*. 2021;19(12):699. doi:10.3390/md19120699
23. Zhu X, Cai J, Wang Y, et al. A high-fat diet increases the characteristics of gut microbial composition and the intestinal damage associated with non-alcoholic fatty liver disease. *Int J Mol Sci*. 2023;24(23):16733. doi:10.3390/ijms242316733
24. Xu J, Bjursell MK, Himrod J, et al. A genomic view of the human-Bacteroides thetaiotaomicron symbiosis. *Science*. 2003;299(5615):2074–2076. doi:10.1126/science.1080029
25. Zhang C, Zhang M, Pang X, et al. Structural resilience of the gut microbiota in adult mice under high-fat dietary perturbations. *ISME J*. 2012;6 (10):1848–1857. doi:10.1038/ismej.2012.27
26. Safari Z, Gérard P. The links between the gut microbiome and non-alcoholic fatty liver disease (NAFLD). *Cell Molec Life Sci*. 2019;76 (8):1541–1558. doi:10.1007/s00018-019-03011-w
27. Che Q, Luo T, Shi J, et al. Mechanisms by which traditional Chinese medicines influence the intestinal flora and intestinal barrier. *Front Cell Infect Microbiol*. 2022;12:863779. doi:10.3389/fcimb.2022.863779

28. Li X, Wu D, Niu J, et al. Intestinal flora: a pivotal role in investigation of traditional Chinese medicine. *Am J Chin Med*. 2021;49(2):237–268. doi:10.1142/S0192415X21500130
29. Hamman JH. Chitosan based polyelectrolyte complexes as potential carrier materials in drug delivery systems. *Mar Drugs*. 2010;8(4):1305–1322. doi:10.3390/md8041305
30. Prandi B, Baldassarre S, Babbar N, et al. Pectin oligosaccharides from sugar beet pulp: molecular characterization and potential prebiotic activity. *Food Funct*. 2018;9(3):1557–1569. doi:10.1039/C7FO01182B
31. Tang D. *Chitosan Improves Obesity by Regulating Intestinal Microbiota and Leptin Levels*. Shandong University; 2020.
32. Bao LK. Characterization of chitosan/pectin polyelectrolyte complex and study of bovine serum protein loading; 2014.
33. Shaabani E, Sharifiaghdam M, De Keersmaecker H, et al. Layer by layer assembled chitosan-coated gold nanoparticles for enhanced siRNA delivery and silencing. *Int J Mol Sci*. 2021;22(2):831. doi:10.3390/ijms22020831
34. Fan Z, Wang C, Yang T, et al. Coffee peel extracts ameliorate non-alcoholic fatty liver disease via a fibroblast growth factor 21-adiponectin signaling pathway. *Food Funct*. 2022;13(13):7251–7259. doi:10.1039/D2FO00081D
35. Jiang J, Yan L, Shi Z, Wang L, Shan L, Efferth T. Hepatoprotective and anti-inflammatory effects of total flavonoids of Qu Zhi Ke (peel of Citrus changshan-huyou) on non-alcoholic fatty liver disease in rats via modulation of NF-κB and MAPKs. *Phytomedicine*. 2019;64:153082. doi:10.1016/j.phymed.2019.153082
36. Tilg H, Moschen AR, Szabo G. Interleukin-1 and inflammasomes in alcoholic liver disease/acute alcoholic hepatitis and nonalcoholic fatty liver disease/nonalcoholic steatohepatitis. *Hepatology*. 2016;64(3):955–965. doi:10.1002/hep.28456
37. Tiegs G, Horst AK. TNF in the liver: targeting a central player in inflammation. *Semin Immunopathol*. 2022;44(4):445–459. doi:10.1007/s00281-022-00910-2
38. Zhang X, Coker OO, Chu ES, et al. Dietary cholesterol drives fatty liver-associated liver cancer by modulating gut microbiota and metabolites. *Gut*. 2021;70(4):761–774. doi:10.1136/gutjnl-2019-319664
39. Kuang J, Wang J, Li Y, et al. Hyodeoxycholic acid alleviates non-alcoholic fatty liver disease through modulating the gut-liver axis. *Cell Metab*. 2023;35(10):1752–1766.e1758. doi:10.1016/j.cmet.2023.07.011
40. Xu Y, Wang N, Tan HY, et al. Panax notoginseng saponins modulate the gut microbiota to promote thermogenesis and beige adipocyte reconstruction via leptin-mediated AMPKα/STAT3 signaling in diet-induced obesity. *Theranostics*. 2020;10(24):11302–11323. doi:10.7150/thno.47746
41. Tremaroli V, Bäckhed F. Functional interactions between the gut microbiota and host metabolism. *Nature*. 2012;489:7415):242–249. doi:10.1038/nature11552
42. Murphy EA, Velazquez KT, Herbert KM. Influence of high-fat diet on gut microbiota: a driving force for chronic disease risk. *Curr Opin Clin Nutr Metab Care*. 2015;18(5):515–520. doi:10.1097/MCO.0000000000000209
43. Lelouvier B, Servant F, Païssé S, et al. Changes in blood microbiota profiles associated with liver fibrosis in obese patients: a pilot analysis. *Hepatology*. 2016;64(6):2015–2027. doi:10.1002/hep.28829
44. Hui D, Liu L, Azami NLB, et al. The spleen-strengthening and liver-draining herbal formula treatment of non-alcoholic fatty liver disease by regulation of intestinal flora in clinical trial. *Front Endocrinol*. 2022;13:1107071. doi:10.3389/fendo.2022.1107071
45. Kirk KF, Nielsen HL, Thorlacius-Ussing O, Nielsen H. Optimized cultivation of Campylobacter concisus from gut mucosal biopsies in inflammatory bowel disease. *Gut Pathog*. 2016;8:27. doi:10.1186/s13099-016-0111-7
46. Liu F, Lee H, Lan R, Zhang L. Zonula occludens toxins and their prophages in Campylobacter species. *Gut Pathog*. 2016;8:43. doi:10.1186/s13099-016-0125-1
47. Konikoff T, Gophna U. Oscillospira: a central, enigmatic component of the human gut microbiota. *Trends in Microbiol*. 2016;24(7):523–524. doi:10.1016/j.tim.2016.02.015
48. Bajaj JS, Betrapally NS, Hylemon PB, et al. Gut microbiota alterations can predict hospitalizations in cirrhosis independent of diabetes mellitus. *Sci Rep*. 2015;5:18559. doi:10.1038/srep18559
49. Zhuang P, Li H, Jia W, et al. Eicosapentaenoic and docosahexaenoic acids attenuate hyperglycemia through the microbiome-gut-organs axis in db/db mice. *Microbiome*. 2021;9(1):185. doi:10.1186/s40168-021-01126-6
50. Zeng SL, Li SZ, Xiao PT, et al. Citrus polymethoxyflavones attenuate metabolic syndrome by regulating gut microbiome and amino acid metabolism. *Sci Adv*. 2020;6(1):eaax6208. doi:10.1126/sciadv.aax6208
51. Liao J, Cao Y, Zhao J, et al. Aqueous extract of Polygala japonica Houtt. ameliorated nonalcoholic steatohepatitis in mice through restoring the gut microbiota disorders and affecting the metabolites in feces and liver. *Phytomedicine*. 2023;118:154937. doi:10.1016/j.phymed.2023.154937